Effect of interstitial oxygen on the crystal structure and magnetic properties of Ni nanoparticles

Aparna Roy, V. Srinivas, S. Ram, J. A. De Toro, and J. M. Riveiro

Citation: Journal of Applied Physics **96**, 6782 (2004); doi: 10.1063/1.1792809
View online: http://dx.doi.org/10.1063/1.1792809
View Table of Contents: http://scitation.aip.org/content/aip/journal/jap/96/11?ver=pdfcov
Published by the AIP Publishing

Effect of interstitial oxygen on the crystal structure and magnetic properties of Ni nanoparticles

Aparna Roy and V. Srinivas[a)]
Department of Physics and Meteorology, Indian Institute of Technology, Kharagpur-721302, India

S. Ram
Material Science Center, Indian Institute of Technology, Kharagpur-721302, India

J. A. De Toro and J. M. Riveiro
Departamento de Fisica Aplicada, Universidad de Castilla-La Mancha, 13071 Ciudad Real, Spain

(Received 24 March 2004; accepted 22 July 2004)

The structure and magnetic properties of fine Ni nanoparticles (~65 nm diameter) having a spontaneous surface oxide layer have been studied. The particles were prepared by the chemical reduction of nickel ions in an aqueous medium, with sodium borohydride as the reducing agent. X-ray diffraction (XRD), transmission electron microscopy, and magnetization measurements (M-H plots and field cooled/zero field cooled curves) have been used for characterizing the samples. No detectable change is observed in the M-H curves or in the XRD patterns of the "as prepared" sample and the sample annealed in air at 573 K. We have indexed both these patterns as Ni in a tetragonal crystal structure with lattice parameters $a=0.4905$ nm, $c=0.5330$ nm and $a=0.4890$ nm, $c=0.5310$ nm for the "as prepared" and 573 K annealed sample, respectively. This is a new report about the formation of Ni in a modified crystal structure. The M-H curves of both the samples show a clear hysteretic behavior but do not saturate, thereby suggesting the existence of both ferromagnetic and paramagnetic components in the magnetization. Large coercivity values ≈ 123 Oe as compared to 6 Oe in bulk Ni have been obtained. The magnetization results have been analyzed in correlation with X-ray diffraction and microstructure and satisfactorily explained on the basis of a core-shell model, where we consider each particle as a magnetically heterogeneous system consisting of a ferromagnetic core of Ni and an antiferromagnetic/paramagnetic shell of NiO. © *2004 American Institute of Physics*. [DOI: 10.1063/1.1792809]

I. INTRODUCTION

Research in the synthesis and functionalization of nanoparticles (NPs) of various sizes and shapes has received considerable interest in recent years because of potential applications in high density magnetic recording media, catalysts, drug delivery systems, ferrofluids, medical diagnostics, solid fuels, and pigments in paints and ceramics.[1,2] The synthesis of nanoscale materials with desired properties is difficult and presents a great challenge to the scientific community. The frequently encountered obstacle is the spontaneous production of oxides. Due to very high surface to volume ratio, nanoparticles have high reactivity and can easily be environmentally degraded. For metal nanoparticles, this results in the NP being encapsulated within a spontaneous surface oxide (SSO) layer, forming what is known as a "core-shell" structure. Nanoparticles having core-shell morphology are of interest in their own right and have been the subject of extensive research in the recent past. For example, in many solar absorbing coatings, the presence of a dielectric shell around at least part of the metallic core, severely delays the oxidation and appears to be the main reason for their good high temperature stability. The oxide close to the metallic core is almost stoichiometric whereas that at the surface consists of atoms with a reduced coordination number. This induces a weakening in the exchange interactions of the surface atoms with the surrounding ones thereby modifying the magnetic and other related properties to an appreciable extent.[3] The SSO shell can behave as antiferromagnetic, paramagnetic, or diamagnetic depending on the nature of the bonding at the surface. Therefore magnetic, optical, and electrical transport characteristics can be tailored by changing the relative dimensions of the core and shell in the NPs. Thus, attempts are being made to synthesize NPs with either SSO or noble metal shells in search of new materials with new properties and applications.

Among the various synthesis techniques, chemical reduction method[4–9] is widely used for producing NPs of Fe, Co, Ni, and their alloys with relatively narrow size distribution. A co-reduction of the transition metal salts by a reducing agent of sodium borohydride ($NaBH_4$), yields the metal or metal borides. However, borohydride reduction chemistry is quite complex and the reaction mechanism differs markedly in aqueous and nonaqueous media. The end product is thus very sensitive to reaction conditions.[4,6,7] Legrand *et al.*[7] attempted to synthesize Ni NPs by chemical reduction method in open air and they identified a mixture of Ni and Ni-B when they analyzed the end product with x-ray photoelectron spectroscopy (XPS). Their sample had no distinct x-ray diffraction peaks of crystalline Ni or Ni-B, except a broad halo characteristic of an amorphous structure at wave

a)Author to whom correspondence should be addressed; FAX:+91-3222-255303; Electronic mail: veeturi@phy.iitkgp.ernet.in

vector $q=31.22\ \text{nm}^{-1}$. On the other hand, Glavee *et al.*[4] reported the formation of both Ni and NiO when the reaction was carried out in aqueous medium under air. It is still not clear what precisely is the reaction mechanism for obtaining the final product as Ni.

In this paper, we investigate the formation of Ni NPs of core-shell structure by coreducing Ni^{2+} ions with $NaBH_4$ in aqueous solution in air. Further we propose a new reaction mechanism and present our new results on the structure of the end product of this method. Subsequently, transformation of ferromagnetic Ni into superparamagnetic NiO is monitored through structural and magnetic properties.

II. EXPERIMENTAL DETAILS

Fine particles of Ni were prepared by reducing the nickel salt $NiCl_2\cdot 6H_2O$ by a reductor of $NaBH_4$, in aqueous solution, at room temperature and ambient atmosphere. 200 ml of a 1.0 Msolution of $NaBH_4$ was added dropwise over a period of 1 h to a 1.0 M $NiCl_2\cdot 6H_2O$ solution in a beaker, with constant magnetic stirring. An instantaneous exothermic reaction ensued with the formation of black slurries of Ni NPs and evolution of H_2 gas. Average temperature of the solution rises by 10–20 K. However, the dropwise addition of $NaBH_4$ controls the reaction and maintains the average temperature of the solution at ~295 K. It seems that the reaction in air monitors *in situ* surface reaction of the resulting Ni sample with H_2O in the solution, forming a stable SSO layer of NiO as an integral part of each individual Ni particle.

After the $Ni^{2+}\rightarrow Ni$ reaction, the sample (slurries of Ni NPs) was filtered and washed thoroughly with distilled water to remove all residual ions from the reaction mixture. This was followed by washing with acetone, to remove the water. A stable surface passivation layer (NiO) developed on drying the recovered powder in vacuum (at ~10 mbar pressure) at room temperature. The sample so obtained is stable in ambient atmosphere. Annealing in air at temperatures of 573, 773, and 973 K for 1 h is used to analyze the oxidative reaction of the Ni core (or the migration of dissolved oxygen) through the NiO shell as diffusion barrier. A pure Ni powder, $NiO+H_2\rightarrow Ni+H_2O\uparrow$, results on annealing the sample in H_2 gas at 973 K or higher temperature.

The crystalline structure of the sample was studied by x-ray diffraction using a P.W. 1718 x-ray diffractometer with filtered Cu Kα radiation of wavelength $\lambda=0.15418$ nm. Microstructure was studied with a JEM 2000 cx transmission electron microscope (TEM). *In situ* elemental analysis with an electron microprobe analyzer confirms the absence of Na^+ and Cl^- byproduct impurities.

The room temperature M-H curves were measured with a vibrating sample magnetometer using magnetic fields upto 14 kOe. The low temperature magnetization measurements [M-H loop at 5 K and field cooled/zero field cooled (FC/ZFC) curves] were taken using a Mag Lab Exa magnetometer (Oxford Instruments) with fields up to 70 kOe and temperatures down to 4 K. The ac susceptibility measurements were done using a home made mutual inductance bridge and a close cycle helium cryostat (Leybold Instruments).

III. RESULTS AND DISCUSSION

A. Reaction process

In the reaction in aqueous solution, a black metal powder of Ni NPs precipitates due to an instantaneous $Ni^{2+}\rightarrow Ni$ coreduction reaction with $NaBH_4$. The reaction occurs in successive steps depending on the initial concentrations of the precursor solutions, the local temperature during the reaction, and other experimental conditions. In a simple form, it can be expressed as

$$NiCl_2 + 2NaBH_4 \rightarrow Ni(BH_4)_2 + 2NaCl, \quad (1)$$

$$Ni(BH_4)_2 + 6H_2O \rightarrow Ni + 2B(OH)_3 + 7H_2\uparrow. \quad (2)$$

The byproduct of $B(OH)_3$ (or boric acid H_3BO_3), which forms *in situ* reconstructive decomposition of the intermediate compound $Ni(BH_4)_2$, coats the resulting Ni particles in a thin surface layer. The excess $B(OH)_3$ remains dissolved in the aqueous solution and does not impart to the final product after the washing process in fresh water. The H_2 gas, which is produced in this reaction, controls a similar reconstructive decomposition of the metastable compound $Ni(OH)_2$, formed by a reaction of nascent Ni NPs with the H_2O[$Ni+2H_2O\leftrightarrow Ni(OH)_2+H_2\uparrow$] during the coreduction process.

A low value of reduction potential[10] $\varphi=-0.87$ V in the reaction $B(OH)_3+3H^++3e\leftrightarrow B+3H_2O$, as compared to $\varphi=-0.257$ V in $Ni^{2+}+2e\leftrightarrow Ni$, favors the hydrolysis reaction of $Ni(BH_4)_2$ with H_2O [Eq. (2)] to form a stable compound $B(OH)_3$. As a result, $B(OH)_3$ once formed in this example does not revert back to metallic boron by reaction with H_2 in aqueous solution. We thus speculate our sample to be relatively free of impurities of metallic boron. A thermal $B(OH)_3\rightarrow 1/2\ B_2O_3+3/2\ H_2O$ decomposition can, however, occur in excessive local heating during the reaction, coating the Ni particles with a rather stable B_2O_3 layer which acts as a diffusion barrier to the reaction species and inhibits growth of the Ni particles during the coreduction process. As a result, as reported earlier by Legrand *et al.*,[7] such a sample presents an amorphous structure with a strong O 1s band in XPS spectrum at 532.8 eV in favorable agreement with a similar band in B_2O_3 at 533.5 eV. The thermal decomposition of $B(OH)_3$, though not completely ruled out, seems less likely in our reaction since care has been taken to keep the local heating during the reaction at a minimum.

Glavee *et al.*[4] reported that an intermetallic compound Ni_2B forms on adding an aqueous solution of $NiCl_2$ to an aqueous solution of $NaBH_4$ in standard inert atmosphere and room temperature over a period of 45 s. A well-defined x-ray diffractogram of an almost single phase Ni_2B occurs after annealing the recovered powder at 673 K in argon gas.[4] The formation of Ni_2B as final product is possibly due to the extremely short reaction time. Here we mention one obvious factor that the spontaneous reaction is rich in the BH_4^- reaction species. Being ionic in nature, the $NaBH_4$ supplies mobile BH_4^- ions as soon as it is added to the $NiCl_2$ solution, so that they react *in situ* primarily with the Ni^{2+} cations and yield $Ni(BH_4)_2$ as an intermediate product [Eq. (1)]. A fast production of $Ni(BH_4)_2$ in large amounts in an extremely fast reaction (45 s in case of Glavee *et al.*) no longer prefers a

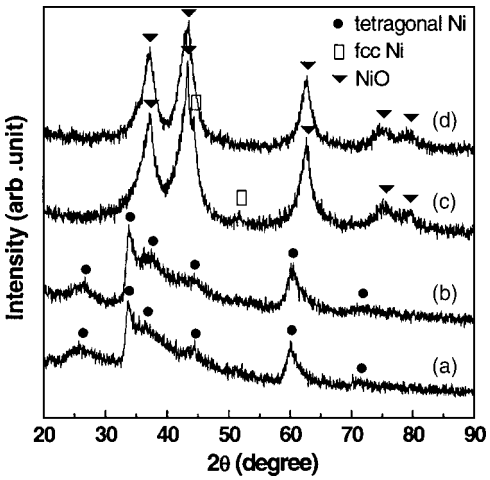

FIG. 1. X-ray diffractograms of "as prepared" sample (a) and after annealing in air at (b) 573 K, (c) 773 K, and (d) 973 K for 1 h. Samples (c) and (d) are reoxidized into NiO nanoparticles.

hydrolysis reaction of it so readily with water. By the time a nascent $Ni(BH_4)_2$ reacts with H_2O it decomposes to a stable Ni_2B compound. A modified coreduction reaction under anaerobic condition and for extremely short reaction time can thus be written as

$$4Ni(BH_4)_2 \rightarrow 2Ni_2B + 6BH_3 + 7H_2\uparrow. \quad (3)$$

subsequently the byproduct BH_3 hydrolyzes in aqueous solution and gives H_2 gas, which maintains a reducing atmosphere, as follows:

$$6BH_3 + 18H_2O \rightarrow 6B(OH)_3 + 18H_2\uparrow. \quad (4)$$

Reaction (3) is, however, unlikely to occur in our experiment as our reaction has been carried out over a long duration of 1 h. It is important to note that Ni borides are better stable against oxidation than pure Ni metal. They hardly react with oxygen at room temperature. So a reaction $4Ni_2B+3O_2 \rightarrow 8Ni+2B_2O_3$, proposed earlier in aqueous solution and air,[4,7,11] showing the conversion of Ni_2B to Ni is not feasible.

During reaction (2) in aqueous solution, some of the OH^- ions get trapped in the growing Ni particles. Possibly a solid solution of Ni, O, and H, viz., $NiO_\beta H_\delta$ then forms by the exchange of electrons present in the reaction medium, with Ni atoms in the lattice. However, since the hydrogen solubility of Ni is very small,[12] the number of H atoms taking part in the solid solution are very few. Nevertheless, the H content defends the sample from internal oxidation reaction with the O atoms, while annealing in air. As regards the solubility of atomic oxygen in metallic Ni, we speculate our sample to contain considerable amounts of dissolved oxygen. This modifies, as analyzed in the following section, the usual $Fm\bar{3}m$ face centered cubic crystal structure[13] of virgin Ni particles and lends credence to our conjecture.

B. X-ray diffraction and microstructure

Figure 1 compares the x-ray diffractograms of (a) "as prepared" Ni powder (dried at room temperature) and those annealed in air at (b) 573 K, (c) 773 K, and (d) 973 K for 1 h. The diffractograms are indicative of a crystalline structure with some degree of amorphosity, the latter being due to the disordered surface layers. No significant changes appear in the diffraction patterns even after annealing the sample at a temperature as high as 573 K. Patterns (a) and (b) do not correspond to face centered cubic (fcc) Ni and no attempts have been made till date by earlier workers[4,7] to identify the structure. After careful analysis, we find that diffraction patterns (a) and (b) are the modified patterns of the usual fcc Ni metal which has space group $Fm\bar{3}m$. The most intense peaks (intensity $I_p=100$ u) in (a) and (b) occur at interplanar spacings of 0.2667 nm and 0.2656 nm, respectively. In the usual Ni metal, the most intense peak (111) lies at $d=0.2034$ nm with the second most intense one (200) at $d=0.1762$ nm ($I_p=42$ u).

The peaks in diffractograms (a) and (b) in Fig. 1 have been indexed assuming a tetragonal crystal structure (Table I) with space group 14/mcm. The lattice parameters are $a=0.4905$ nm, $c=0.5330$ nm for the "as prepared" sample and $a=0.4890$ nm, $c=0.5310$ nm for the sample annealed at 573 K. We propose that a tetragonal Ni-O_β lattice is derived from the fcc Ni lattice by the incorporation of O atoms at the interstitial positions of the latter. The presence of these oxygen atoms, which have larger atomic radii (1.40 Å) compared to Ni (1.246 Å), strains the Ni lattice and makes it tetragonal. As shown in Fig. 2(a), in the proposed unit cell of tetragonal Ni, the O atoms replace part of the Ni atoms in the family of ⟨001⟩ planes in the usual fcc Ni lattice. It adds a new crystallographic plane of (002) with one O atom at the

TABLE I. X-ray diffraction pattern of Ni nanocrystals of tetragonal crystal structure. The lattice parameters are given below. "As prepared" powders: $a=0.4905$ nm; $c=0.5330$ nm. 573 K annealed powders: $a=0.4890$ nm; c=0.5310 nm.

As prepared			573 K Annealed		
d_{hkl} (nm)[a]	Intensity[b]	(*hkl*)	d_{hkl} (nm)[a]	Intensity[b]	(*hkl*)
0.3466 (0.3468)	33	(110)	0.3440 (0.3458)	32	(110)
0.2667 (0.2665)	100	(002)	0.2656 (0.2655)	100	(002)
0.2455 (0.2452)	77	(200)	0.2436 (0.2445)	71	(200)
0.2038 (0.2029)	57	(211)	0.2036 (0.2022)	50	(211)
0.1544 (0.1551)	67	(310)	0.1538 (0.1546)	67	(310)
0.1322 (0.1318)	20	(321)	0.1316 (0.1314)	18	(321)

[a]The figures in parentheses are the d_{hkl} values, calculated from the respective lattice parameters of the samples.
[b]The relative intensities are normalized assuming 100 u of intensity for the most intense peak.

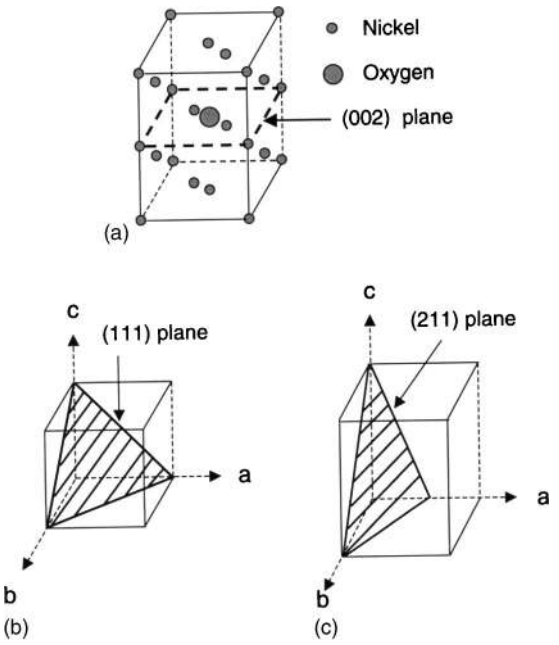

FIG. 2. (a) A model unit cell of tetragonal Ni with an oxygen atom at the center. The incorporation of the O atom modifies the (b) (111) plane of FCC Ni into (c) (211) plane.

center as marked in the diagram. The characteristic (111) plane of fcc Ni [Fig. 2(b)] gets modified to (211) plane [Fig. 2(c)] in accordance with the x-ray diffraction pattern. The unit cell has a total of eight atoms, one O atom and seven Ni atoms, and gives a density value of $\rho=5.527$ g/cm^3 for the "as prepared" sample and $\rho=5.582$ g/cm^3 for the sample annealed at 573 K. Consistently the value is improved to 8.910 g/cm^3 as in fcc Ni after desorbing the oxygen by annealing the sample at 973 K in H_2 gas (Fig. 3). Although no peaks of NiO are observed in patterns (a) and (b), it is quite probable that the oxide layers in these samples are in an amorphous state.

The O atoms in Ni-O_β become mobile at temperatures above 573 K and when annealed in air, induce phase transformation according to the equation

$$\text{Ni-O}_\beta = \text{cubic} - \text{Ni}_{1-\beta} + \beta\text{NiO}. \tag{5}$$

The c-Ni appears with recrystallized NiO [Fig. 1(c)] on annealing in air at 773 K. Tetragonal Ni thus remains stable till 573 K, i.e., as long as O atoms remain dissolved in the lattice and keep it strained. An efficient reaction with O_2 from air occurs on annealing at 973 K, resulting in the formation of fine NiO particles of crystallite size 4.5 nm, as estimated from x-ray diffraction line broadening [Fig. 1(d)] using Scherrer equation.

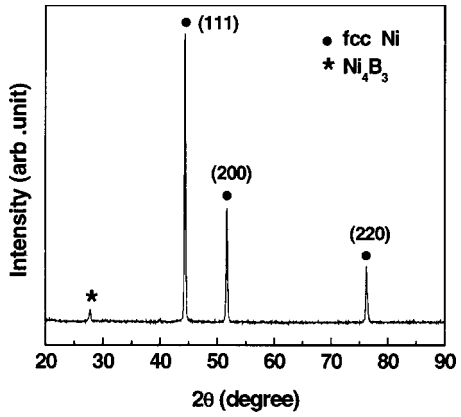

FIG. 3. X-ray diffractogram of fcc nickel powder, obtained after annealing the "as prepared" powder in H_2 gas at 973 K for 1 h. A faint Ni_4B_3 (111) peak is also seen.

Aggregated, spherical particles of average diameter 66.6 nm are seen in the TEM micrographs (Fig. 4) of the metal powder, before annealing (a) and after annealing at 573 K (b). Figure 4(c) represents a close up of the sample obtained after controlled oxidative reaction in air at 973 K. It shows ultrafine particles of NiO of median size 11 nm, clustered together to form one big particle. Here, both the core and shell consists of NiO. Possibly, an amorphous structure retains in shell. The electron diffractogram (d) of this sample has five distinct rings at d_{hkl} values 2.417, 2.080, 1.481, 1.250, and 1.201 Å. All five rings are due to NiO with reflections from (111), (200), (220), (311), and (222) planes, in favorable agreement with the x-ray diffraction values.

C. Magnetic properties

The magnetic state of the "as prepared" and annealed samples has been assessed through room temperature magnetization data. Figure 5 shows the M-H curves of the "as prepared," and the 573 K annealed sample at room temperature (300 K). A clear ferromagnetic component as indicated by hysteresis (inset) is present, with coercivity (H_c) and remanent magnetization (M_r) values of 123.86 Oe, 0.1088 emu/g, and 120.64 Oe, 0.0869 emu/g, respectively. The magnetization of these samples is found not to saturate. As evident from the initial magnetization curves (Fig. 6), the magnetization at lower fields shows a rapid increase with field, followed by a curvature and then by a linear behavior suggesting the existence of two different magnetic phases in each particle—a ferromagnetic and a paramagnetic phase. The first is responsible for the rapid increase of the magnetization at low fields while the second is responsible for the nonsaturation of the magnetization at higher fields. Each particle can thus be considered as a magnetically heterogeneous system consisting of a ferromagnetic Ni core and an outer shell of NiO and any other paramagnetic impurities in the form of nickel borides. However, no significant borides could be detected in the XRD patterns even after annealing in air at 973 K for 1 h, though a very faint peak of Ni_4B_3 appears in the sample annealed in H_2 gas.

An attempt to separate the ferromagnetic and paramagnetic components from the initial magnetization curves has been made (Fig. 6 inset) by expressing the total magnetization of a particle in the high field region (few thousand oersteds) as

$$M(H) = M_s(1 - \alpha/H) + \chi H, \tag{6}$$

where M_S is the saturation magnetization, χ is the paramagnetic susceptibility, and "α" is a constant, generally interpreted as due to inclusions and/or microstress.[14] Reasonably good fits of Eq. (6) to the high field region of the initial magnetization curves have been obtained, with M_S values of 0.4476 and 0.3592 emu/g and χ values of 3×10^{-5} and 4

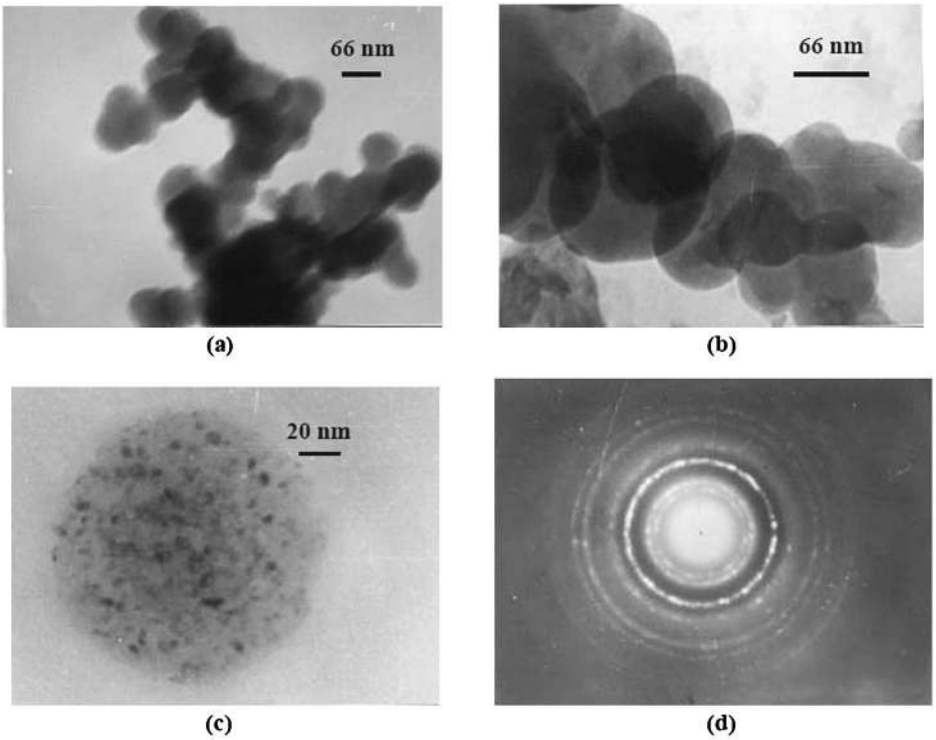

FIG. 4. TEM micrographs of "as prepared" sample (a) and after annealing in air at (b) 573 K, and (c) 973 K. (d) is the electron diffraction pattern of sample (c).

$\times 10^{-5}$ emu/g Oe for "as prepared" and 573 K annealed samples, respectively. Our attempts to fit more complicated functions suggested by earlier workers[15] to the complete initial magnetization curve gave better fits but resulted in unphysical values of χ. The small values of M_S as compared to 54.39 emu/g in bulk Ni are due to the presence of surface layers which are either spin disordered (canted moments in the oxide coating) or magnetically dead.[16,17] It is also noticed that the magnetization decreases slightly when the sample is annealed in air at 573 K. This is due to the increase in oxide layer thickness which (oxide) though imperceptible from XRD pattern, is most likely to be present in an amorphous state.

The coercivity values (~120 Oe at room temperature) of "as prepared" and 573 K annealed samples are two orders of magnitude higher than the value of 6 Oe for bulk Ni. This cannot be due to small particle dimensions alone. We attribute this to the influence of interface anisotropy which through exchange coupling can modify the magnetism of the core. The Ni core and NiO shell nanostructure can be described as a magnetic bilayer with spherical geometry. It is then reasonable to anticipate that the NiO shell acts as a pinning layer as in spin valve structures, pinning the core spins near the interface of the Ni core and NiO shell via exchange interactions. This prevents the core spins from rotating freely in commensurate with the applied field, thereby leading to large observed coercivities. The first few layers of the NiO shell just surrounding the Ni core are antiferromagnetic and act as the pinning layers while at the surface the

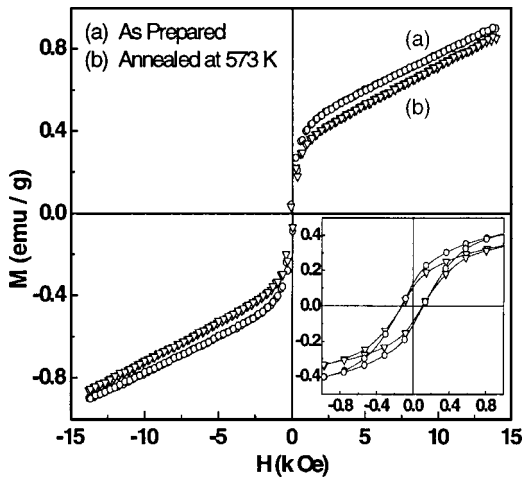

FIG. 5. Magnetization as a function of applied at 300 K for (a) "as prepared" and (b) 573 K annealed sample. The inset gives an expanded view of the plots and clearly shows hysteresis.

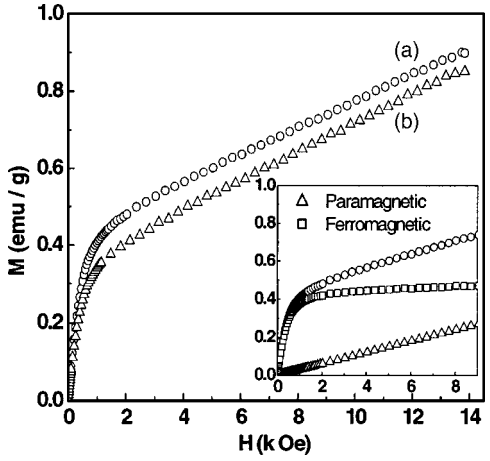

FIG. 6. Initial magnetization curves of (a) "as prepared" and (b) 573 K annealed sample. The inset shows the separated components for the "as prepared" sample with (□) and (Δ) as the ferromagnetic and paramagnetic components, respectively.

TABLE II. The core diameter and shell thickness of "as prepared" and 573 K annealed samples as estimated from magnetization data and XRD pattern.

Sample	[a]Density ρ (g/cm^3)	Total diameter d_{total} (from TEM) (nm)	M_s emu/g	d_{core} (nm)	t_{shell} (nm)	Crystallite size of Ni (from XRD) (nm)
As prepared	5.527	66.66	0.448	14.321	26.173	11.979
Annealed at 573 K	5.582	66.82	0.359	13.266	26.872	10.864

[a]The ρ values are for tetragonal Ni.

spins are uncompensated, misaligned, and without any magnetic order. It is these randomly oriented spins which align with increase in field and give rise to the paramagnetic component χH.

The Ni core diameter (d_{core}) and NiO shell thickness (t_{shell}) for "as prepared" and 573 K annealed samples were determined from the magnetization data on similar considerations as in Ref. 16. The core diameters are in good agreement with the crystallite sizes obtained for Ni from the "slow scanned" XRD patterns of the samples. Table II gives a summary of the results.

Figure 7 shows the room temperature M-H curve of the sample annealed in air at 973 K. The absence of a ferromagnetic component in this sample is consistent with the XRD results, i.e., the fine particles are completely oxidized into NiO. The crystallite size of these particles as estimated from XRD line broadening using Scherrer equation is 4.5 nm. The room temperature M-H curve of this sample (Fig. 7) fits well to the Langevin function, yielding an average particle moment of 1322 μ_B and saturation magnetization of 1.6 emu/g. Thus as per the simple Langevin theory of paramagnetism, our sample can be considered to consist of noninteracting, magnetic particles, but clustered together as is evident from [Fig. 4(c)]. The reasonably good Langevin fit clearly suggests that the particles are superparamagnetic at room temperature. We have also estimated the particle size from the fitting parameters (particle moment and saturation magnetization) of the Langevin function, assuming the particles to be perfectly NiO with a density of 6.67 g/cm^3. It is ~12 nm, in close agreement with the value of 10 nm obtained from TEM measurements. It is interesting to point out that the *M-H* data for NiO NPs as reported by Makhlouf *et al.*[18,19] had to be fit to a modified Langevin function containing an extra linear term. The same observation was reported by Biasi *et al.*[3] for ultrafine Fe-Ni-B nanoparticles. The reason for the inclusion of the linear term has not been explained. The inset of Fig. 7 shows the initial magnetization curve of this sample, measured at $T=5$ K. The magnetization does not saturate even at such low temperature and high field of 60 k Oe. The presence of large high field susceptibility at 5 K is an indication of strong magnetic anisotropy in the sample and is interpreted in terms of surface and interface effects.

The temperature dependence of the magnetization of the above sample has been studied through the FC and ZFC curves, measured at a constant dc field of 100 Oe (Fig. 8). They exhibit the typical blocking process of an assembly of superparamagnetic particles, with an average blocking temperature $T_B=120$ K. This is defined as a temperature at which the ZFC curve exhibits a maximum. The ZFC peak is wide, hinting at a distribution of relaxation times because of a distribution in particle size. As ac susceptibility (ACS) measurements provide independent information about T_B, the

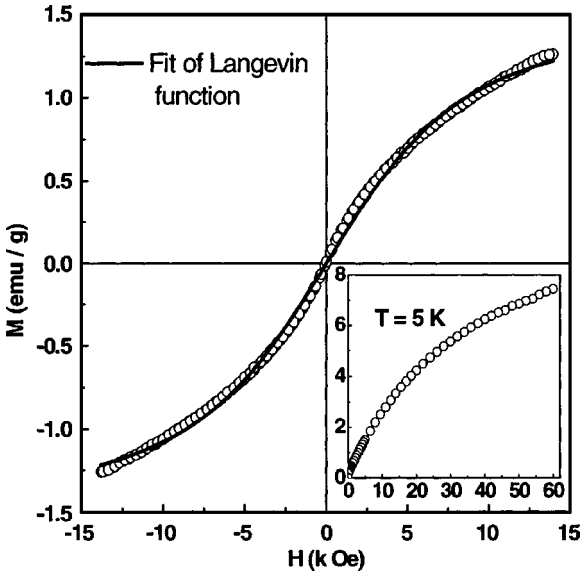

FIG. 7. Magnetization as a function of applied field at 300 K, for the 973 K annealed (in air) sample. The solid line is the fit of the Langevin function to the data. The inset shows the initial magnetization curve of this sample at 5 K.

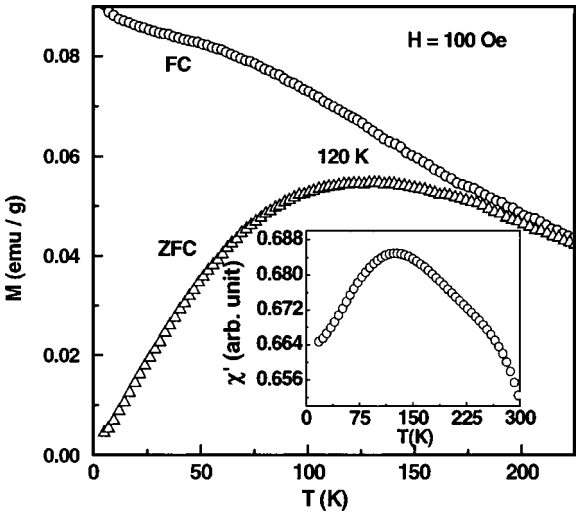

FIG. 8. Magnetization of FC and ZFC NiO particles (973 K annealed sample) in 100 Oe applied field, as a function of temperature. Inset: Real part of ac susceptibility vs temperature.

real component χ' of ACS is plotted as a function of temperature (Fig. 8 inset) for an applied ac field of 2 Oe and frequency 80 Hz. It shows a peak close to 120 K in close conformity with magnetization data.

IV. CONCLUSIONS

Fine particles of oxide coated Ni have been synthesized using the borohydride reduction method. The XRD pattern has been indexed as Ni in a tetragonal crystal structure. The formation of tetragonal Ni is due to the presence of dissolved oxygen in the Ni lattice. When the sample is annealed at 973 K in argon or hydrogen gas, FCC nickel was obtained due to the desorption of the dissolved oxygen. Small M_s but large H_c values are due to the pinning of the Ni core spins by the NiO shell. The magnetization data could be satisfactorily explained on the basis of core-shell geometry of the particles.

[1]E. Matijevic, Mater. Res. Bull. **14**, 19 (1989).
[2]M. Ozaki, Mater. Res. Bull. **14**, 35 (1989).
[3]E. D. Biasi, C. A. Ramos, R. D. Zysler, and H. Romero, Phys. Rev. B **65**, 144416 (2002).
[4]G. N. Glavee, K. J. Klabunde, C. M. Sorensen, and G. C. Hadjipanayis, Langmuir **10**, 4726 (1994).
[5]D. A. Van Leeuwen, J. M. Van Ruitenbeck, L. J. De Jonyh, A. Ceriotti, G. Pacchioni, O. D. Haberlen, and R. Rosch, Phys. Rev. Lett. **73**, 1432 (1994).
[6]J. P. Chen, C. M. Sorensen, K. J. Klabunde, and G. C. Hadjipanayis, Phys. Rev. B **51**, 11527 (1995).
[7]J. Legrand, A. Taleb, S. Gota, M. J. Guittet, and C. Petit, Langmuir **18**, 4131 (2002).
[8]J. Park and J. Cheon, J. Am. Chem. Soc. **123**, 5743 (2001).
[9]S. Ram and P. S. Frankwickz, Phys. Status Solidi A **188**, 1129 (2001).
[10]*CRC Handbook of Chemistry and Physics*, 72 ed. Chap. 8, pp. 17–20.
[11]G. N. Glavee, K. J. Klabunde, C. M. Sorensen, and G. C. Hadjipanayis, Inorg. Chem. **32**, 474 (1994).
[12]K. Zeng, T. Klassen, W. Oelerich, and R. Bormann, J. Alloys Compd. **283**, 151 (1999).
[13]X-ray Powder Diffraction File JCPDS-ICDD (Joint Committee on Powder Diffraction Standards-International Centre for Diffraction Data, Swarthmore, PA) 04–850 Ni.
[14]B. D. Cullity, *Introduction to Magnetic Materials* (Addison-Wesley, Reading, MA 1972), p. 347.
[15]W.-N. Wang, G.-X. Cheng, and Y.-W. Du, J. Magn. Magn. Mater. **153**, 11 (1996).
[16]P. Zhang, F. Zuo, F. K. Urban, A. khabari, P. Griffiths, and A. Hosseini-Tehrani, J. Magn. Magn. Mater. **225**, 337 (2001).
[17]S. Gangopadhyay, G. C. Hadjipanayis, B. Dale, C. M. Sorensen, K. J. Klabunde, V. Papaefthymiou, and A. Kostikas, Phys. Rev. B **45**, 9778 (1992).
[18]S. A. Makhlouf, F. T. Parker, F. E. Spada, and A. E. Berkowitz, J. Appl. Phys. **81**, 5561 (1997).
[19]R. H. Kodama, S. A. Makhlouf, and A. E. Berkowitz, Phys. Rev. Lett. **79**, 1393 (1997).